

This article appeared in a journal published by Elsevier. The attached copy is furnished to the author for internal non-commercial research and education use, including for instruction at the authors institution and sharing with colleagues.

Other uses, including reproduction and distribution, or selling or licensing copies, or posting to personal, institutional or third party websites are prohibited.

In most cases authors are permitted to post their version of the article (e.g. in Word or Tex form) to their personal website or institutional repository. Authors requiring further information regarding Elsevier's archiving and manuscript policies are encouraged to visit:

<http://www.elsevier.com/authorsrights>



ash. Several literatures have reported the total contents of heavy metals in the bottom ash. For example, Chimenos et al. (Chimenos et al., 1999) studied the total contents of Pb, Zn, Cu, Mn, Sn, Cr, Ni and Cd in the size fractionated bottom ash. However, the determination of the total contents of heavy metals in bottom ash is unable to provide sufficient information to understand the environmental impact (Qu et al., 2008). The mobility of the heavy metals is greatly related to their specific chemical forms and binding states (Gleyzes et al., 2002). In this respect, the sequential extraction procedure (SEP) is of great importance. It is more than a relatively simple tool in relating heavy metals to mineralogical species. It also gives detail information about their mobilization and bioavailability. Some researchers have adopted the SEP to explore the chemical property of the heavy metals in the bottom ash. E.g. Zhao et al. (Zhao et al., 2008) used the SEP to investigate the fractionation of the rare earth elements in the bottom ash. Yao et al. (Yao et al., 2010a, 2010b) used the SEP to reveal the fractionation and mobility of Cd, Co, As, Cr, Cu, Mn, Mo, Ni, Pb and Zn in the bottom ash. However, the fractionation of the heavy metals in the size fractionated bottom ash has been rarely reported. As the bottom ash is likely to be used according to the particles sizes, it is important to investigate the fractionation of heavy metals in the size fractionated bottom ash.

In this study, the MSWI bottom ash was divided into six classes: < 0.45 mm, 0.45–1 mm, 1–2 mm, 2–4 mm, 4–8 mm and > 8 mm. The total contents and fractionation distribution of the Cu, Zn and Cd in the size fractionated MSWI bottom ash were investigated. Cu was selected to represent the lithophilic metals, Zn for the moderately volatile metals, and Cd for the volatile metals. It aims to provide scientific reference for the pollution control of MSWI bottom ash utilization.

## 2. Materials and methods

### 2.1. Sampling and sieving

MSWI bottom ash sample was taken from Green Energy MSWI plant in Zhejiang province, East China (Fig. 1). The plant consisted of three parallel stoker

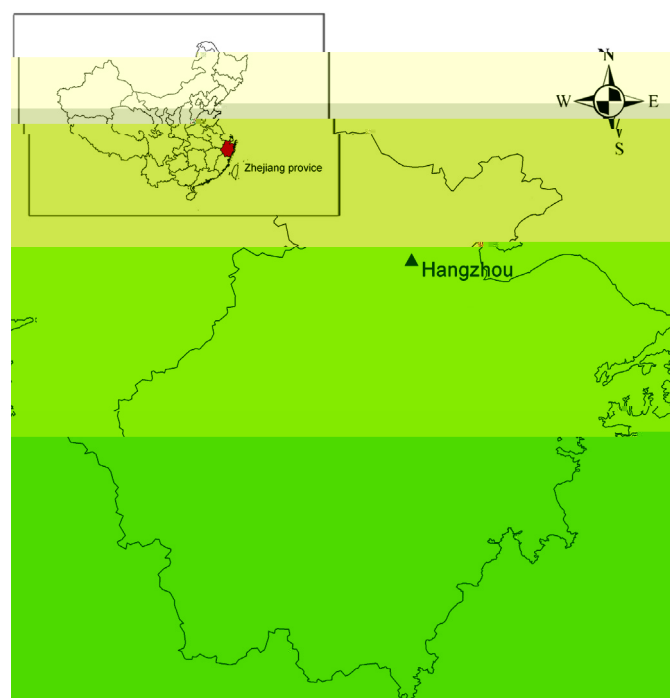


Fig. 1. Map of sampling location.

incinerators with a MSW treatment capacity of 650 t/d, which was equipped with the wet extraction system for the bottom ash. The source MSW was collected from several residential areas of Hangzhou without any industrial solid waste. The operating temperature of the incinerators was 850–1100 °C, and the residence time of the waste in the incinerator was about 50 min. Bottom ash was immediately sampled after it is produced, cooled and magnetically separated. The sampling period lasted for 5 days. Approximately 25 kg of the fresh bottom ash sample was taken daily from the plant. Totally, a 125 kg bottom ash sample was obtained. The bottom ash sample was stored in a hermetically closed container for a week. Then the bottom ash sample was manually mixed by the shovel to homogenize it.

The sieving of the bottom ash was carried out by shaking with stainless steel mesh screens to particle size classes of < 0.45 mm, 0.45–1 mm, 1–2 mm, 2–4 mm, 4–8 mm and > 8 mm, respectively. To determine the contents and fractionation of the heavy metals, as well as the physical–chemical properties, 100 g sample was taken for the different particle size classes of the bottom ash.

### 2.2. Bulk composition and physical–chemical properties analysis

The contents of individual elements in the bottom ash sample were analyzed after the sample was digested according to the method described by Yamasaki (1997). 0.5 g of air dried sample was weighed into a Teflon beaker. 2.5 mL HNO<sub>3</sub> and 2.5 mL HClO<sub>4</sub> were added and heated at 150 °C for 2–3 h. After cooling, 2.5 mL HClO<sub>4</sub> and 5 mL HF were added and heated at 150 °C for 15 min, and then 5 mL HF was added until the residue became almost dry. The residue was dissolved using 5 mL HNO<sub>3</sub> and diluted to 100 mL. The element concentrations in the solution were determined by ICP-OES (Thermo Electron Corporation IRIS/AP, USA). The samples were digested and analyzed in triplicate.

The loss on ignition (LOI), including LOI<sub>600 °C</sub> and LOI<sub>950 °C</sub> were determined by heating the bottom ash samples at 600 °C and 950 °C respectively, according to the Chinese standard GB7876–87. The value of (LOI<sub>600 °C</sub> – moisture content) indirectly reflected the organic matter content in MSWI bottom ash, while the value of (LOI<sub>950 °C</sub> – LOI<sub>600 °C</sub>) reflected the content of carbonate minerals. All the measurements were conducted in triplicate.

### 2.3. Sequential Extraction Procedure (SEP)

The fractionation of Cu, Zn and Cd in the bottom ash sample was determined by using SEP suggested by Tessier et al. (1979). It was performed according to the following procedure:

Exchangeable (F1): 2.0 g of bottom ash was added with 16 mL of magnesium chloride solution (1 M MgCl<sub>2</sub>, pH 7.0) and shaken for 1 h at room temperature;

Bound to carbonate (F2): The residue from the exchangeable fraction was shaken with 16 mL of 1 M CH<sub>3</sub>COONa (pH 5.0) for 5 h at room temperature;

Bound to Fe–Mn oxides (F3): 20 mL of 0.04 M hydroxylamine hydrochloride (NH<sub>2</sub>OH · HCl) in 25% (v/v) CH<sub>3</sub>COOH was added to the residue from the carbonate fraction and heated at 96 ± 1 °C for 5 h with occasional agitation;

Bound to organic matters (F4): 6 mL of 0.02 M HNO<sub>3</sub> and 10 mL of 30% hydrogen peroxide (H<sub>2</sub>O<sub>2</sub>) (pH 2.0) were added to the residue from the Fe–Mn oxides fraction and heated at 85 ± 1 °C for 2 h with occasional agitation. Another aliquot of 6 mL 30% hydrogen peroxide (H<sub>2</sub>O<sub>2</sub>) (pH 2.0) was added and heated again at 85 ± 1 °C for 3 h with intermittent agitation. After cooling to room temperature, 10 mL of 3.2 M ammonium acetate (CH<sub>3</sub>COONH<sub>4</sub>) in 20% HNO<sub>3</sub> was added and agitated continuously for 30 min;

Residual fraction (F5): The residual fraction was determined by digestion of residue from the fraction bound to organic matters, as described in Section 2.2.

The SEP was conducted in triplicate and heavy metal concentrations in the solutions of each step were determined by ICP-OES (Thermo Electron Corporation IRIS/AP, USA).

## 3. Results and discussion

### 3.1. Size distribution of the bottom ash

The size distribution of the bottom ash was illustrated in Fig. 2 (a). It showed a unimodal distribution, with the highest peak located at the particle size of 4–8 mm. A higher mass percentage of weight was observed in the bottom ash with large particle sizes. The individual mass percentage of the particle size of 2–4 mm, 4–8 mm and > 8 mm was higher than 19%, while the individual mass percentage of the particle size of < 0.45 mm, 0.45–1 mm and 1–2 mm was all below 15%. Generally, the bottom ash could be divided into two categories: (1) the incineration slag of the MSW, including the inert substance unable to burn; and (2) the grate sifting precipitated from the furnace wall during the incineration.

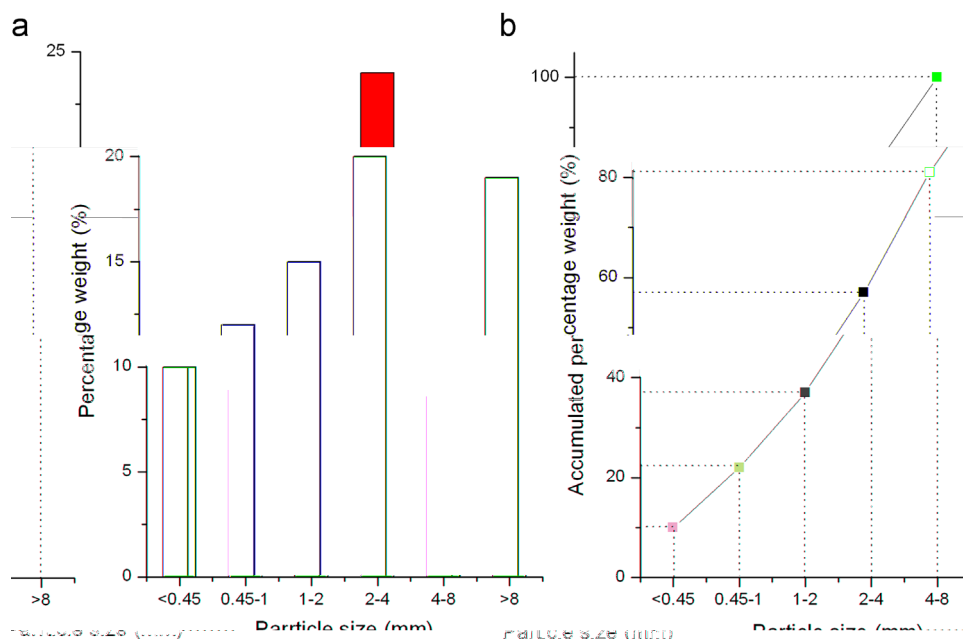


Fig. 2. Size distribution of the MSWI bottom ash.

The slag is usually presented in the large particle size while the grate sifting normally in the fine size. The results indicated that the major proportion of the bottom ash was from the incineration slag.

According to the size distribution of the bottom ash, the cumulative mass percentage for the bottom ash was obtained, as shown in Fig. 2(b). The mass median diameter ( $d_{50}$ ) can be determined, which was 3.25 mm. Furthermore, the geometric standard deviation ( $\sigma_g$ ) calculated from  $(d_{84}/d_{16})^{1/2}$  was 3.82, where  $d_{84}$  and  $d_{16}$  represented the diameters at 84% and 16%, respectively.

### 3.2. Particle distribution of heavy metals

The particle distribution of Cu was shown in Fig. 3(a). The highest content of Cu in the bottom ash was observed in the particle size of > 8 mm, which was 1452.4 mg/kg dry wt. The bottom ash with the particle size of 4–8 mm and < 0.45 mm had a comparable content of Cu, which was 594.3 and 597.0 mg/kg dry wt., respectively. The bottom ash with the particle sizes of 0.45–1 mm, 1–2 mm and 2–4 mm had a relatively low level of Cu, which was below 450 mg/kg dry wt. It was thought that the bottom ash with the particle size higher than 4 mm was mainly from the incineration slag, while the bottom ash with the particle size of < 0.45 mm was generally from the grate sifting. The heavy metals in the slag usually had not gone through the evaporation process in the furnace, while the heavy metals in the fine ash might be transferred to the raw gas and subsequently precipitated homogeneously. The high content of Cu in the bottom ash with the particle size of > 4 mm indicated that a considerable amount of Cu was kept in the matrix of the incineration slag without the evaporation process. This result could also be supported by the high variation of the Cu content in the large ash (Fig. 3(a)). However, the relatively high content of Cu was also found in the bottom ash with the particle size of < 0.45 mm, which was inconsistent with the lithophilic property of Cu (Verhulst and Buekens, 1996). It might be attributed to the function of the 'entrainment of the particle matrix', which meant some of the Cu in the MSW was entrained by the raw gas and precipitated with the fine ash afterwards. This result could also be proved by the

fractionation of the Cu in the fine ash, which would be discussed in the Section 3.3.

The content of Zn showed a relatively even distribution among the various particles compared with that of Cu, which ranged from 1567 (> 8 mm) to 1754 mg/kg dry wt. (< 0.45 mm), with the average content of 1708.5 mg/kg dry wt. (Fig. 3(b)). The high content of Zn in the bottom ash was probably due to the high content of Zn in MSW, as observed by several previous studies (Long et al., 2009a, Long et al., 2009b). The content of Zn was slightly higher in the fine ash, which was consistent with the thermodynamic characteristic of Zn. As is known, Zn has a moderate volatility. The volatility of Zn was higher than that of Cu, but lower than that of Cd. It started to form  $ZnCl_2(g)$  when the temperature was above 280 °C, and twenty percent of Zn was assumed to be volatilized at 800 °C (Verhulst and Buekens, 1996). The moderate volatility of Zn resulted in its relatively even distribution and the slight higher content in the fine ash.

The content of Cd was relatively low compared to that of Cu and Zn. However, due to the high toxicity of Cd, it still needed to be concerned. The content of Cd ranged from 13.4 to 23.4 mg/kg dry wt. (Fig. 3(c)). The highest content of Cd was observed in the particle size of 0.45–1 mm. The content of Cd in the fine ash (< 1 mm) was generally higher than that in the large ash, which was consistent with the result of Chimenos et al. (Chimenos et al., 1999). This result was not surprising as Cd was a volatile element. It starts to volatilize at 300 °C and the volatilization is complete at 400 °C (Verhulst and Buekens, 1996). It suggested most of the available Cd in the MSW would be transferred to the raw gas under the furnace condition, which was above 850 °C. The high content of Cd in the fine ash was probably due to the precipitation of Cd from the raw gas, which was rich in Cd.

Generally, bottom ash contained a high level of Cu, Zn and Cd. The size distribution of these metals greatly depended on the thermodynamic characteristic and transfer behavior of the metal species. The high content of Cu was found in both the fine and the large ash, which was due to its lithophilic character and entrainment within the particle matrix. Zn showed an even distribution due to its moderate volatility. The content of Cd was higher in the fine ash because of its high volatility.

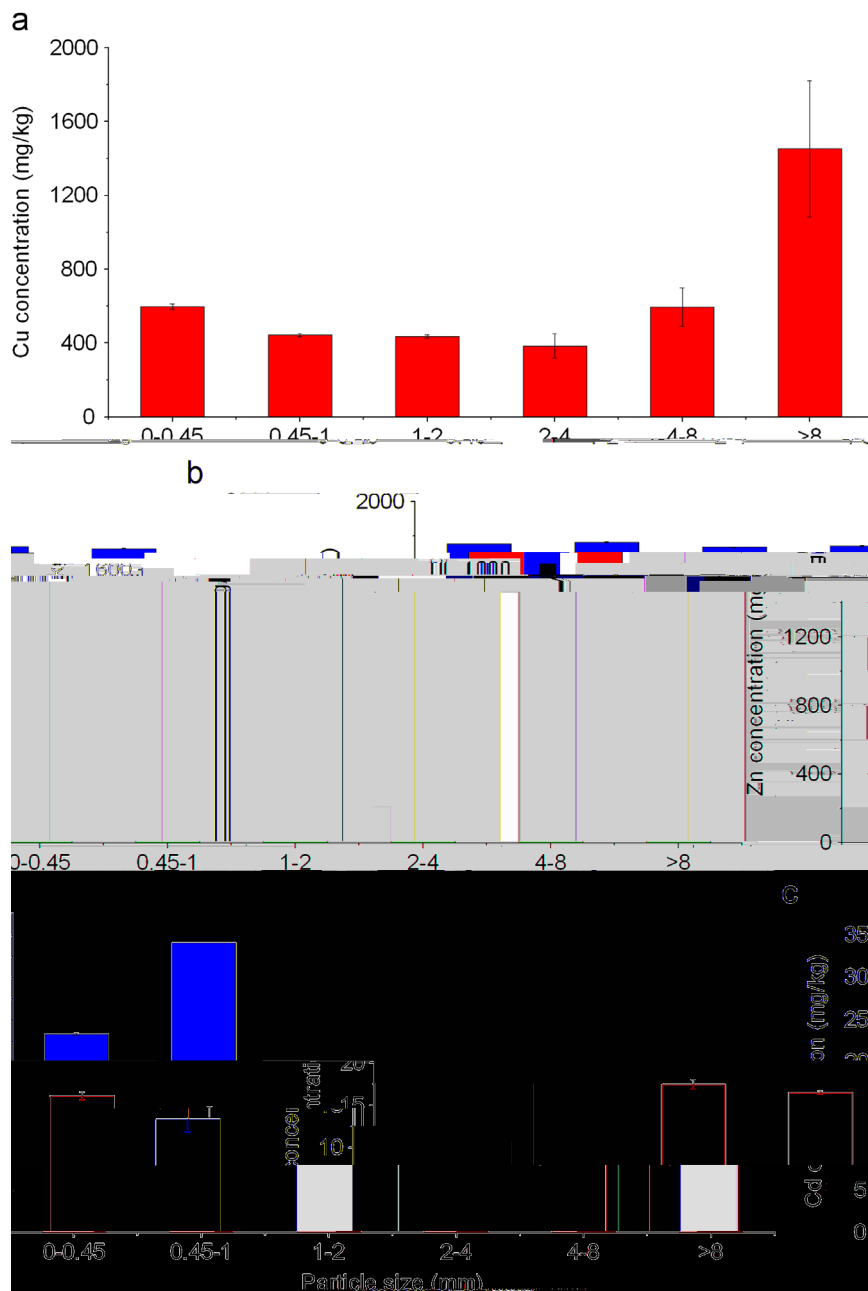


Fig. 3. Contents of Cu, Zn and Cd in the size fractionated MSWI bottom ash.

### 3.3. Fractionation of heavy metals in the bottom ash

The sequential fractionation of Cu, Zn and Cd in the size fractionated bottom ash was exhibited in Fig. 4. Cu was mainly presented as the residual fraction for all the particle sizes of bottom ash, which accounted for 69.2%, 64.6%, 66.3%, 68.7%, 62.0% and 56.4% for the particle size of < 0.45 mm, 0.45–1 mm, 1–2 mm, 2–4 mm, 4–8 mm and > 8 mm, respectively (Fig. 4(a)). It indicated that the mass ratio of the residual fraction showed a decreasing trend with the increase of the particle size. The mass ratio of the organic matter bound fraction of Cu was higher than other species, due to its high affinity with the organic matter, such as humic substance (Olsson et al., 2007). Generally, the mass ratio of the organic matter bound of Cu increased with the increase of the particle size. It accounted for 21.0% for the particle size of < 0.45 mm and it achieved 33.7% for the particle size > 8 mm. This result was corresponding to the content of organic

matter in the various particle sizes (Fig. 5(a)). The incomplete combustion of the incineration slag resulted in the relatively high level of the organic matter in the large ash, while the fine ash was mainly from raw ash containing a low level of organic matter. The high level of organic matter provided better opportunity for the complexation of the Cu with the organic matter. The Fe–Mn oxide bound fraction of Cu showed an even distribution, which ranged from 2.2% to 3.6%. The carbonate bound fraction showed an upward trend with the increase of the particle sizes. This result was surprising as the fine ash has a better opportunity to interact with CO<sub>2</sub> in the furnace, thus it should have a relatively high content of carbonate bound fraction of Cu (Fig. 5(b)). This result further proved that the Cu in the fine ash was mainly from the entrainment of the particle matrix, other than evaporation. Moreover, the exchangeable fraction of Cu decreased when the particle size increased. It suggested that the fine ash had more easily soluble Cu in the surface.



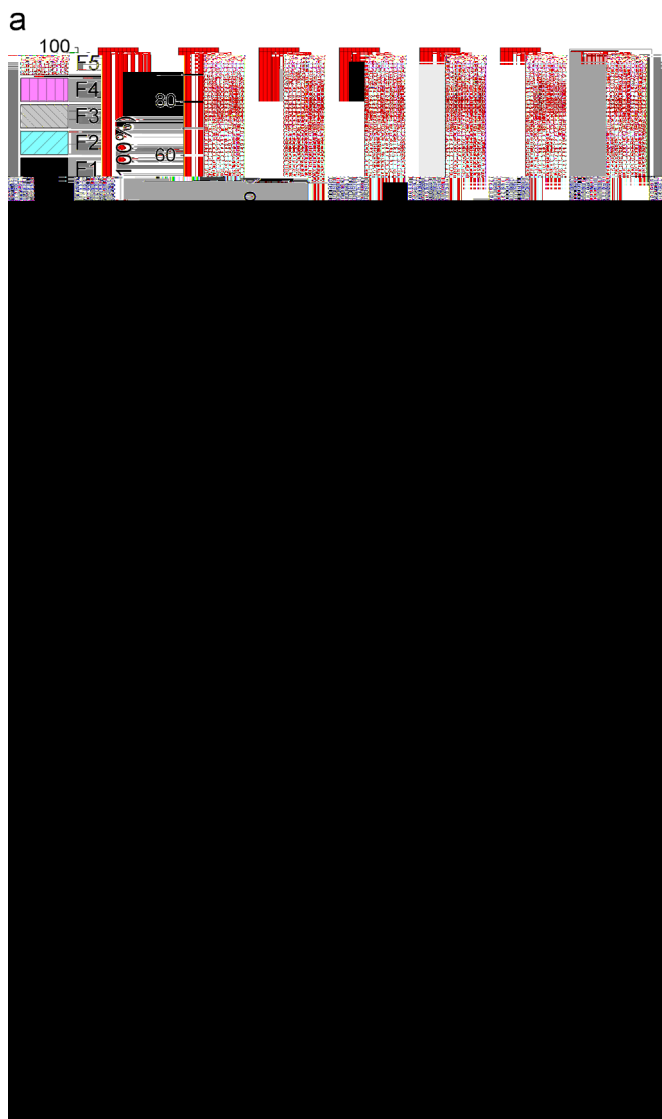


**Fig. 4.** Fractionation of Cu, Zn and Cd in the size fractionated MSWI bottom ash. F1: exchangeable fraction; F2: carbonate bound fraction; F3: Fe–Mn oxide bound fraction; F4: organic matter bound fraction and F5: residual fraction.

The residual fraction of Zn showed a slight increase from 67.7% to 71.1% with the increase of the particle size. Meanwhile, the organic matter bound fraction of Zn showed a decreasing trend with the increase of the particle size, which ranged from 4.1% to 7.9%. No significant difference was observed for the Fe–Mn oxide bound fraction and carbonate bound fraction among the various particle sizes, ranging from 11.4% to 13.0% and 11.3% to 13.0%, respectively. Besides, the exchangeable fraction of Zn was minimal, ranging from 0.16% to 0.27%. Generally speaking, the fractionation of Zn showed a more even distribution among the ash with different particle sizes than that of Cu and Cd.

Compared with Cu and Zn, Cd showed a high mass percentage of the exchangeable fraction and carbonate bound fraction. The mass percentage of the exchangeable fraction of Cd in the ash ranged from 8.3% to 17.6%, which increased with the increase of the particle size. The mass percentage of the carbonate bound fraction of Cd showed a decreasing trend, ranging from 20.6% to 31.3%. This result was distinct from that of Cu, but was consistent with the intrinsic property of Cd as a volatile element. Most of the Cd in the fine ash was from the evaporation. The evaporated Cd was able to interact with  $\text{CO}_2$ , forming the carbonate bound fraction. Besides, the Fe–Mn oxide bound fraction of Cd decreased

when the particle size increased. The organic matter bound fraction of Cd did not show an obvious trend, whose content ranged 4.6%–8.3%. The residual fraction of Cd showed a decreasing trend, ranging from 34.3% to 47.9%.

The results showed that the fractionation of Cu, Zn and Cd varied among the different size particles, and was greatly depended on the intrinsic property of the metal species and their transfer behavior in the furnace. The lithophilic metal Cu showed completely different sequential fractionation distribution compared with the volatile metal Cd.

### 3.4. Implication

The exchangeable fraction and carbonate bound fraction are considered as the unstable fraction under the acidic condition (Gleyzes et al., 2002; Maiz et al., 2000; Udovic and Lestan, 2009). These fractions are apt to leach out when the pH is low. Unfortunately, more and more areas have become the acid rain region. For example, the pH of the rain in the Southeastern China is usually lower than 4.0 (Zhang et al., 2007). In such an acidic condition, the exchangeable fraction and carbonate bound fraction of the metals are assumed to be leached out from the bottom ash. In the term of environmental protection, the total amounts of the exchangeable fraction and carbonate bound fraction of Cu, Zn and Cd in the size fractionated bottom ash were calculated, as illustrated in Table 1. Furthermore, the Fe–Mn oxide bound fraction has the potential bioavailability under the anoxic condition, and the organic matter bound fraction is unstable under the oxidizing condition (Tessier et al., 1979). Therefore, the total amounts of the exchangeable fraction, carbonate bound fraction and Fe–Mn oxide bound fraction, as well as the total amounts of the exchangeable fraction, carbonate bound fraction and organic matter bound fraction of Cu, Zn and Cd in the various particle sizes of bottom ash were also calculated (Table 1), in case the bottom ash was reused in the acidic anoxic or acidic oxidizing condition.

According to the Table 1, the highest unstable amounts were observed in the large ash for Cu. Zn showed a relatively even distribution of unstable amounts among the particle sizes. The fine ash contained the highest unstable amounts of Cd. Several studies argued that the pollution threat of fine ash would be more serious than that of the large ash due to its high specific surface area, which allowed the fine ash to capture more pollutants (Chimeno et al., 1999; Hjelmar, 1996). However, the results of the present study indicated the large ash of the bottom ash could also be a serious pollution source, especially for the lithophilic heavy metals. In this respect, special attention should be paid to the lithophilic heavy metals when the large ash is re-utilized. Meanwhile, special attention should be paid to the volatile heavy metals when the fine ash is reused.

## 4. Conclusions

The contents and fractionation of Cu, Zn and Cd in the MSWI bottom ash with different particle sizes were investigated. The results revealed that both the contents and the fractionation of the metals varied among the different particle sizes, which were related to the thermodynamic characteristic and transfer behavior of the metals. The volatile metal Cd showed a decreasing trend with the increase of the particle size due to the evaporation process. Moreover, Cd in the fine ash was apt to be present in the carbonate-bound fraction, due to the interaction of  $\text{CO}_2$  and Cd during evaporation process. On the contrary, the lithophilic element Cu showed a different distribution pattern. A higher fraction of Cu was presented as the organic matter bound fraction in the large ash than the fine ash, as the large ash contained more

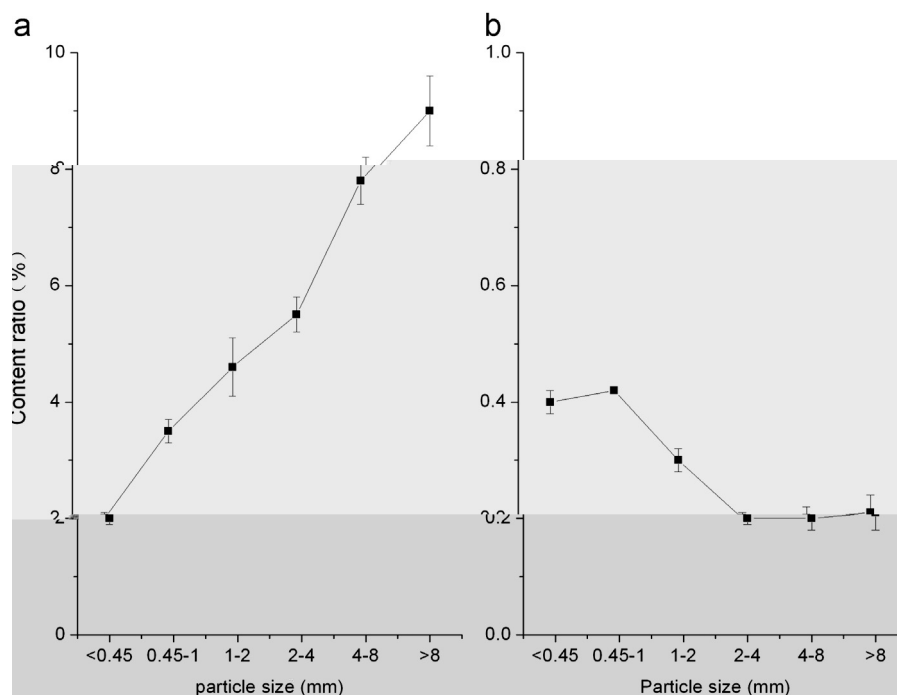


Fig. 5. Value of (LOI<sub>600</sub>)

organic matter. The present study also suggested that the large ash contained more unstable lithophilic metals than the fine ash, while the fine ash contained more unstable volatile metals than the large ash. Therefore, special attention should be paid to the lithophilic heavy metals when the large ash is re-utilized while volatile heavy metals deserve more concern when the fine ash is reused.

### Acknowledgments

This work was financially supported by Natural Science Foundation of Zhejiang province with Grant no. LQ13B070001 and Open Foundation of Zhejiang Provincial Key Laboratory of Solid Waste Treatment and Recycling Grant no. SWTR-2012-06.

### References

- Belevi, H., Moench, H., 2000. Factors determining the element behavior in municipal solid waste incinerators. 1. Field studies. *Environ. Sci. Technol.* 34, 2501–2506.
- Belevi, H., Langmeier, M., 2000. Factors determining the element behavior in municipal solid waste incinerators. 2. Laboratory experiments. *Environ. Sci. Technol.* 34, 2507–2512.
- Chang, Y.H., Chen, W.C., Chang, N.B., 1998. Comparative evaluation of RDF and MSW incineration. *J. Hazard. Mater.* 58, 33–45.
- Chimenos, J.M., Segarra, M., Fernández, M.A., Espiell, F., 1999. Characterization of the bottom ash in municipal solid waste incinerator. *J. Hazard. Mater.* 64, 211–222.
- Gleyzes, C., Tellier, S., Astruc, M., 2002. Fractionation studies of trace elements in contaminated soils and sediments: a review of sequential extraction procedures. *TrAC—Trends Anal. Chem.* 21, 451–467.
- Hjelmar, O., 1996. Disposal strategies for municipal solid waste incineration residues. *J. Hazard. Mater.* 47, 345–368.
- Long, Y.Y., Hu, L.F., Fang, C.R., He, R., Shen, D.S., 2009a. Releasing behavior of zinc in recirculated bioreactor landfill. *Sci. Total Environ.* 407, 4110–4116.
- Long, Y.Y., Hu, L.F., Jiang, C.J., Fang, C.R., Wang, F.P., Shen, D.S., 2009b. Releasing behavior of copper in recirculated bioreactor landfill. *Bioresour. Technol.* 100, 2419–2424.
- Maiz, I., Arambarri, I., García, R., Millán, E., 2000. Evaluation of heavy metal availability in polluted soils by two sequential extraction procedures using factor analysis. *Environ. Pollut.* 110, 3–9.
- National Bureau of Statistics of China, 2009. *China Statistical Yearbook*. China Statistical Press, Beijing.
- Olsson, S., van Schaik, J.W.J., Gustafsson, J.P., Kleja, D.B., van Hees, P.A.W., 2007. Copper(II) binding to dissolved organic matter fractions in municipal solid waste incinerator bottom ash leachate. *Environ. Sci. Technol.* 41, 4286–4291.
- Qu, X., He, P.J., Shao, L.M., Lee, D.J., 2008. Heavy metals mobility in full-scale bioreactor landfill: initial stage. *Chemosphere* 70, 769–777.
- Tessier, A., Campbell, P.G.C., Bisson, M., 1979. Sequential extraction procedure for the speciation of particulate trace metals. *Anal. Chem.* 51, 844–851.
- Udovic, M., Lestan, D., 2009. Pb, Zn and Cd mobility, availability and fractionation in aged soil remediated by EDTA leaching. *Chemosphere* 74, 1367–1374.

- Verhulst, D., Buekens, A., 1996. Thermodynamic behavior of metal chlorides and sulfates under the conditions of incineration furnaces. *Environ. Sci. Technol.* 30, 50–56.
- Wan, X., Wang, W., Ye, T.M., Guo, Y.W., Gao, X.B., 2006. A study on the chemical and mineralogical characterization of MSWI fly ash using a sequential extraction procedure. *J. Hazard. Mater.* 134, 197–201.
- Yamasaki, S., 1997. Digestion methods for total analysis. In: Japanese Society of Soil Science and Plant Nutrition. *Soil Environment Analysis*, Tokyo, Hakuyusya.
- Yao, J., Li, W.B., Kong, Q.N., Wu, Y.Y., He, R., Shen, D.S., 2010a. Content, mobility and transfer behavior of heavy metals in MSWI bottom ash in Zhejiang province, China. *Fuel* 89, 616–622.
- Yao, J., Li, W.B., Kong, Q.N., Xia, F.F., Shen, D.S., 2012. Effect of weathering on the mobility of zinc in municipal solid waste incinerator bottom ash. *Fuel* 93, 99–104.
- Yao, J., Li, W.B., Tang, M.L., Fang, C.R., Feng, H.J., Shen, D.S., 2010b. Effect of weathering treatment on the fractionation and leaching behavior of copper in municipal solid waste incinerator bottom ash. *Chemosphere* 81, 571–576.
- Youcai, Z., Lijie, S., Guojian, L., 2002. Chemical stabilization of MSW incinerator fly ashes. *J. Hazard. Mater.* 95, 47–63.
- Zhang, H., He, P.J., Shao, L.M., 2008. Fate of heavy metals during municipal solid waste incineration in Shanghai. *J. Hazard. Mater.* 156, 365–373.
- Zhang, M.Y., Wang, S.J., Wu, F.C., Yuan, X.H., Yin, Zhang, 2007. Chemical compositions of wet precipitation and anthropogenic influences at a developing urban site in southeastern China. *Atmos. Res.* 84, 311–322.
- Zhao, L.J., Zhang, F.S., Zhang, J.X., 2008. Chemical properties of rare earth elements in typical medical waste incinerator ashes in China. *J. Hazard. Mater.* 158, 465–470.